CD9 shapes glucocorticoid sensitivity in pediatric B-cell precursor acute lymphoblastic leukemia

Chi Zhang,[1] Kathy Yuen Yee Chan,[1] Wing Hei Ng,[1] John Tak Kit Cheung,[1] Qiwei Sun,[1] Han Wang,[1] Po Yee Chung,[1] Frankie Wai Tsoi Cheng,[2] Alex Wing Kwan Leung,[1] Xiao-Bing Zhang,[3] Po Yi Lee,[1] Siu Ping Fok,[1] Guanglan Lin,[1] Ellen Ngar Yun Poon,[4] Jian-Hua Feng,[5] Yan-Lai Tang,[6] Xue-Qun Luo,[6] Li-Bin Huang,[6] Wei Kang,[7] Patrick Ming Kuen Tang,[7] Junbin Huang,[8] Chun Chen,[8] Junchao Dong,[9] Ester Mejstrikova,[10] Jiaoyang Cai,[11] Yu Liu,[11] Shuhong Shen,[11] Jun J Yang,[12] Patrick Man Pan Yuen,[1] Chi Kong Li[1,13] and Kam Tong Leung[1,13]

[1]Department of Paediatrics, The Chinese University of Hong Kong, Shatin, Hong Kong; [2]Department of Paediatrics and Adolescent Medicine, Hong Kong Children's Hospital, Kowloon Bay, Hong Kong; [3]Haihe Laboratory of Cell Ecosystem, Institute of Hematology & Blood Diseases Hospital, Tianjin, China; [4]School of Biomedical Sciences, The Chinese University of Hong Kong, Shatin, Hong Kong; [5]Department of Hematology, The First Affiliated Hospital of Wenzhou Medical University, Wenzhou, China; [6]Department of Pediatrics, The First Affiliated Hospital, Sun Yat-sen University, Guangzhou, China; [7]Department of Anatomical and Cellular Pathology, The Chinese University of Hong Kong, Shatin, Hong Kong; [8]Division of Hematology/Oncology, Department of Pediatrics, The Seventh Affiliated Hospital, Sun Yat-sen University, Shenzhen, China; [9]Department of Immunology, Zhongshan School of Medicine, Sun Yat-sen University, Guangzhou, China; [10]CLIP-Department of Pediatric Hematology and Oncology, Second Faculty of Medicine, Charles University and University Hospital Motol, Prague, Czech Republic; [11]Department of Hematology/Oncology, Shanghai Children's Medical Center, School of Medicine, Shanghai Jiao Tong University, Shanghai, China; [12]Department of Pharmaceutical Sciences, St. Jude Children's Research Hospital, Memphis, TN, USA and [13]Hong Kong Hub of Paediatric Excellence, The Chinese University of Hong Kong, Shatin, Hong Kong

Correspondence: K.T. Leung
ktleung@cuhk.edu.hk

Received: February 15, 2023.
Accepted: March 22, 2024.
Early view: April 4, 2024.

https://doi.org/10.3324/haematol.2023.282952

Abstract

Resistance to glucocorticoids (GC), the common agents for remission induction in pediatric B-cell precursor acute lymphoblastic leukemia (BCP-ALL), poses a significant therapeutic hurdle. Therefore, dissecting the mechanisms shaping GC resistance could lead to new treatment modalities. Here, we showed that CD9^{-} BCP-ALL cells were preferentially resistant to prednisone and dexamethasone over other standard cytotoxic agents. Concordantly, we identified significantly more poor responders to the prednisone prephase among BCP-ALL patients with a CD9^{-} phenotype, especially for those with adverse presenting features including older age, higher white cell count and *BCR-ABL1*. Furthermore, gain- and loss-of-function experiments dictated a definitive functional linkage between CD9 expression and GC susceptibility, as demonstrated by the reversal and acquisition of relative GC resistance in CD9^{low} and CD9^{high} BCP-ALL cells, respectively. Despite physical binding to the GC receptor NR3C1, CD9 did not alter its expression, phosphorylation or nuclear translocation but potentiated the induction of GC-responsive genes in GC-resistant cells. Importantly, the MEK inhibitor trametinib exhibited higher synergy with GC against CD9^{-} than CD9^{+} lymphoblasts to reverse drug resistance *in vitro* and *in vivo*. Collectively, our results elucidate a previously unrecognized regulatory function of CD9 in GC sensitivity, and inform new strategies for management of children with resistant BCP-ALL.

Introduction

Acute lymphoblastic leukemia (ALL) is the most common childhood hematologic malignancy, accounting for ~25% of pediatric cancers.[1] The classical treatment protocol comprises sequential phases of remission induction, consolidation, delayed intensification and maintenance, which relies on the risk-directed usage of multiagent therapy including the backbone drugs prednisolone (Pred), dexamethasone (Dex), vincristine (VCR), L-asparaginase

(L-ASP), cytarabine (Ara-C), daunorubicin (DNR), methotrexate (MTX) and 6-mercaptopurine (6-MP).[2] Optimal application of these agents, together with refined risk group stratification and appropriate supportive care, has yielded a significant improvement in the overall survival of newly diagnosed pediatric ALL to over 85% in most developed countries.[3,4] However, disease relapse still occurs in 10-20% of patients, with <50% of whom can be cured with salvage regimens, indicating the emergence of drug resistance and requirement for treatment interventions.[5,6] Glucocorticoids (GC), including Pred and Dex, are the core therapeutic agents for remission induction in pediatric ALL. In some treatment protocols, patients with a poor response to the Pred prephase were stratified into the high-risk arm to receive intensified multiagent chemotherapy.[7–10] Resistance to GC is found in 15-30% of newly diagnosed pediatric ALL cases and 70% of relapsed patients.[11] Moreover, specific high-risk subtypes of ALL, including those with *KMT2A* rearrangements or *BCR-ABL1* translocation, tend to have poorer responses to GC.[12,13] GC induce apoptosis in malignant lymphoblasts by binding to the glucocorticoid receptor NR3C1. This ligand-activated transcription factor subsequently undergoes phosphorylation, translocates into the nucleus and activates the transcription of GC-responsive genes.[14] Diverse mechanisms have been reported to attribute resistance of ALL to GC, including but not limited to mutations of the GC receptor NR3C1[15] and co-activator CREBBP,[16] alteration of molecular signaling pathways, such as MAPK,[17] NOTCH1,[18] AKT[19] or AURKB,[20] and deregulation of the BCL-2 family protein BIM.[21] Indeed, the reversal of GC resistance has been considered a potential intervening strategy for further improvement of patient outcomes and is especially important for relapsed ALL.[22] Preclinical investigations have revealed early successes, as demonstrated by the restoration of GC sensitivity in T-cell ALL by the AKT inhibitor MK2206[23] and in B-cell precursor (BCP)-ALL by the MEK1/2 inhibitor trametinib.[17] While some of these agents are scheduled to be evaluated in upfront clinical trials, it is important to further investigate new mechanisms underlying GC resistance, and leverage the knowledge to develop intervening strategies for high-risk subjects.

CD9, a prototypic member of the tetraspanin family proteins, is involved in many physiologic processes, such as cell migration and adhesion, by forming complexes with other transmembrane or cytosolic proteins into a membrane structure known as the tetraspanin-enriched microdomain (TEM), where the functions of partner proteins are modulated.[24] Substantial evidence also reveals the importance of CD9 in solid and hematologic malignancies, although its nature is context-dependent and cannot be strictly classified as an oncogene or tumor suppressor.[25] Our group previously identified CD9 as a critical effector of hematopoietic stem cell homing[26] and recently also unleashed its prognostic significance in pediatric BCP-ALL.[27,28] In order to elucidate whether its impact on clinical outcome is related to drug response, we, in this study, further profiled the sensitivity pattern of $CD9^+$ and $CD9^-$ BCP-ALL to frontline therapeutic agents, and discovered its previously unknown linkage with GC susceptibility.

Methods

Full experimental procedures are described in the *Online Supplementary Appendix*.

Cells, patient cohort and CD9 characterization

BCP-ALL cell lines were maintained in serum-supplemented RPMI-1640 medium. $CD9^{low}$ cells were transduced with control GFP-only or CD9-GFP lentiviral particles to achieve gene overexpression, whereas $CD9^{high}$ cells were transduced with control sgRNA-Cas9-GFP or CD9 sgRNA-Cas9-GFP to achieve gene knockout.[29] Primary lymphoblasts were recovered from diagnostic samples of pediatric BCP-ALL cases consecutively recruited into three successive clinical studies,[7–9] where patients were unanimously treated with a Berlin-Frankfurt-Münster (BFM)-based protocol with a Pred prephase. All human specimens were obtained with informed written consent and in accordance with procedures approved by the Joint CUHK-NTEC Clinical Research Ethics Committee. Lymphoblasts were characterized for CD9 expression by flow cytometry, with gating strategy shown in *Online Supplementary Figure S1A*.

Drug sensitivity assay

BCP-ALL cell lines were treated with dimethyl sulfoxide (DMSO) or 0.1 nM to 100 μM of Pred, Dex, Ara-C, DNR, VCR, or MTX for 72 hours. Cell proliferation was measured by MTS assay. A mesenchymal stem cell (MSC)-based drug testing system was adopted to determine the sensitivity of primary lymphoblasts to GC.[30] Representative flow cytometry plots showing the sequential gating for defining apoptotic lymphoblasts are shown in *Online Supplementary Figure S1B*. The half-maximal inhibitory concentrations (IC_{50}) were calculated from the dose-response curves by nonlinear regression.[31] In some experiments, BCP-ALL cells were concomitantly treated with the indicated doses of trametinib or ruxolitinib to determine their synergy with GC using the Bliss independence model.[32]

Western blotting and co-immunoprecipitation

Whole cell lysates or subcellular components were recovered from BCP-ALL cells with or without GC treatment. Proteins were separated and detected for CD9, NR3C1, p-NR3C1, MEK1/2, p-MEK1/2, ERK1/2 or p-ERK1/2 by standard SDS-PAGE and immunoblotting procedures. In order to dictate protein-protein interactions, lysates were immunoprecipitated with CD9 antibody and probed for NR3C1 or TEM components.[24]

RNA sequencing, chromatin immunoprecipitation sequencing and quantitative real-time polymerase chain reaction

Total RNA was extracted from patient samples or BCP-ALL cell lines with or without Dex treatment. cDNA libraries were generated and sequenced to curate GC-responsive genes, *NR3C1* isoform expression and *NR3C1* hotspot mutations.[33,34] Chromatin of Dex-treated BCP-ALL cells was precipitated with NR3C1 antibody. Eluted DNA fragments were sequenced to locate and quantify NR3C1 binding.[35] Quantitative real-time polymerase chain reaction (RT-PCR) was performed with TaqMan-based assays to validate selected GC-responsive genes (*Online Supplementary Table S1*).

Xenograft experiments

Animal experiments were conducted in accordance with procedures approved by the Institutional Animal Experimentation Ethics Committee. NSG mice were infused with luciferase-expressing $CD9^{low}$ SEM or $CD9^{high}$ BV-173 cells. On day 3 post-transplantation, animals were randomized to receive a 2-week treatment of vehicle control, Dex (5 mg/kg), trametinib (5 mg/kg) or their combination.[36] At humane endpoints, systemic and bone marrow leukemic load were measured by bioluminescence imaging and flow cytometry, respectively.

Statistical analyses

The statistical methods applied for individual experiments are indicated in the table footnotes or figure legends. Analyses were performed with GraphPad Prism v8.3.0 or SPSS v26.0. *P* values of <0.05 were considered statistically significant.

Results

B-cell precursor acute lymphoblastic leukemia cells with low CD9 expression are resistant to glucocorticoids

In order to investigate the association of CD9 expression with drug response, we first performed *in vitro* sensitivity profiling of $CD9^{high}$ (697, BV-173, RS4;11 and SUP-B15; cell surface CD9 expression higher than mean) and $CD9^{low}$ BCP-ALL cell lines (KOPN-8 and SEM; cell surface CD9 expression lower than mean) to standard therapeutic agents used in remission induction or consolidation therapy for pediatric BCP-ALL (Figure 1A). Hierarchical clustering analyses revealed distinct drug sensitivity patterns and a clear association with CD9. In cluster A, the BCP-ALL cells, in general, were sensitive to Ara-C, DNR, VCR or MTX, without significant differences in the extent of drug responses between $CD9^{high}$ and $CD9^{low}$ lines. In cluster B, which exclusively contained the two tested GC, $CD9^{high}$ but not $CD9^{low}$ lines were sensitive to Pred (mean IC_{50}: 140 *vs.* 19,357 nM, *P*=0.015) or Dex (mean IC_{50}: 9.0 *vs.* 693 nM; *P*=0.002). We then validated the impact of CD9 on GC responses using primary cells isolated from 18 diagnostic BCP-ALL samples encompassing the major cytogenetic subtypes, with patient characteristics shown in *Online Supplementary Table S2*. Concordantly, under a MSC co-culture system, lymphoblasts from $CD9^{+}$ cases exhibited markedly higher sensitivity to Pred (median IC_{50}: 269 *vs.* 8,186 nM; *P*=0.03) or Dex (median IC^{50}: 31.5 *vs.* 2,761 nM; *P*=0.03) when compared to $CD9^{-}$ cases (Figure 1B, C).

CD9 negativity is associated with poor prednisone responses in B-cell precursor acute lymphoblastic leukemia patients

We then capitalized on our three clinical studies,[7-9] which commonly adopted a treatment prephase of 7-day Pred before the initiation of multi-agent chemotherapy, to retrospectively explore the association of CD9 with early GC responses in pediatric BCP-ALL. A total of 182 children (median age, 4.4 years) were recruited, stratified into $CD9^{+}$ and $CD9^{-}$ subgroups (positivity defined by the presence of ≥20% $CD9^{+}$ blasts; this cutoff consistently showed the strongest prognostic significance in our single- and multi-center studies),[27,28] and compared for Pred responses (poor response defined by the presence of $\geq 1\times10^{9}$/L circulating leukemic blasts on day 8).[8] In this cohort, 16 patients (8.8%) were poor prednisone responders (Table 1). Consistent with the *ex vivo* drug testing results, more $CD9^{-}$ patients exhibited poor responses to Pred than $CD9^{+}$ patients (19.4% *vs.* 6.2%; *P*=0.02). Subgroup analyses further revealed that poor Pred responders with a $CD9^{-}$ phenotype were significantly enriched in patients with older age (60% *vs.* 3.7%; *P*=0.008), male sex (21.7% *vs.* 6.7%; *P*=0.045), higher white cell count (66.7% *vs.* 15.4%, *P*=0.004) and in those with *BCR-ABL1* translocation (100% *vs.* 12.5%; *P*=0.024) or not otherwise specified BCP-ALL (30.8% *vs.* 5.8%; *P*=0.019). Notwithstanding, there was no significant enrichment of $CD9^{-}$ patients in these high-risk subgroups (*Online Supplementary Table S3*). Univariate analyses revealed that $CD9^{-}$ phenotype, high white cell count and the presence of *BCR-ABL1* were significantly associated with poor Pred responses. Multivariate analyses further confirmed CD9 negativity as an independent predictive factor for this adverse feature (odds ratio [OR]=5.1, *P*=0.009; *Online Supplementary Table S4*).

CD9 is definitively linked to glucocorticoid susceptibility

In order to validate the association of CD9 with GC sensitivity at the functional level, we first employed a gain-of-function approach by transducing $CD9^{low}$ SEM cells with GFP or CD9-GFP lentiviral vectors, resulting in control $GFP^{+}CD9^{low}$ and experimental $GFP^{+}CD9^{high}$ stable cell lines (Figure 2A). We then tested their sensitivity to standard therapeutic agents. Convincingly, $CD9^{high}$ SEM cells ex-

hibited 8.9- and 2.8-fold increases in sensitivity to Pred (IC_{50}: 6,231 *vs.* 55,346 nM; *P*=0.017) or Dex (IC_{50}: 351 *vs.* 991 nM; *P*=0.005), respectively when compared with control $CD9^{low}$ cells (Figure 2B). Such differential drug sensitivity was not observed for other cytotoxic agents, except for a modest increase in the sensitivity of $CD9^{high}$ SEM cells to Ara-C (Figure 2C). Similar findings were observed in another $CD9^{low}$ cell line KOPN-8, where experimental $GFP^{+}CD9^{high}$ cells exhibited 23.5- and 203-fold increases in sensitivity to Pred (IC_{50}: 2,260 *vs.* 53,195 nM; *P*=0.003)

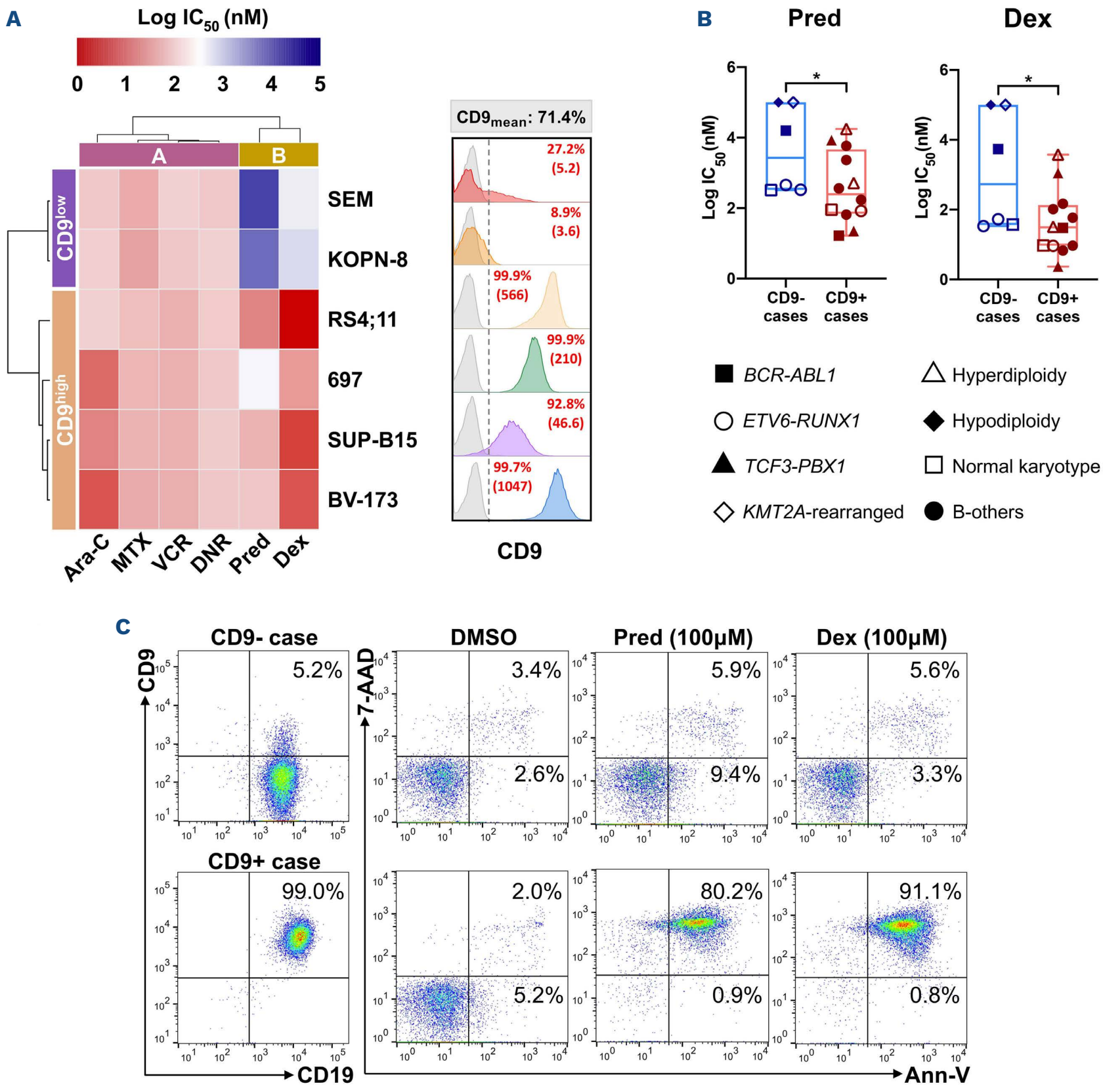

Figure 1. Drug sensitivity profiling reveals preferential resistance of $CD9^{low}$ B-cell precursor acute lymphoblastic leukemia cells to glucocorticoids. (A, left) Heatmap showing the responses of B-cell precursor acute lymphoblastic leukemia (BCP-ALL) cell lines to standard therapeutic agents. The color scale delineates the log_{10} half-maximal inhibitory concentration (IC_{50}) range. Cluster A, drugs without differential activities between $CD9^{high}$ and $CD9^{low}$ cells. Cluster B, drugs with differential activities between $CD9^{high}$ and $CD9^{low}$ cells. (A, right) Flow histograms showing cell surface CD9 expression on individual BCP-ALL cell lines. The percentages of $CD9^{+}$ populations and mean fluorescense intensity (MFI) (numbers in bracket) are indicated. The mean CD9 expression is shown on the top and was used define CD9 status. (B) *Ex vivo* responses of $CD9^{-}$ (N=6) and $CD9^{+}$ (N=12) BCP-ALL samples to prednisolone (Pred) or dexamethasone (Dex). Cytogenetic features of individual samples are annotated. Statistics: two-tailed, unpaired Student's *t* test. *$P<0.05$. (C) Representative flow cytometry plots showing the levels of apoptotic lymphoblasts of $CD9^{+}$ and $CD9^{-}$ cases after treatment with 100 μM Pred or Dex for 96 hours in mesenchymal stem cell (MSC) co-cultures. Ara-C: cytarabine; DNR: daunorubicin; VCR: vincristine; MTX: methotrexate.

Table 1. Association of CD9 with prednisone response in pediatric B-cell precursor acute lymphoblastic leukemia.

Prednisone response	All patients N=182		CD9⁺ patients N=146		CD9⁻ patients N=36		CD9⁺ *vs.* CD9⁻
	Good	Poor	Good	Poor	Good	Poor	*P*
Whole cohort, N (%)	166 (91.2)	16 (8.8)	137 (93.8)	9 (6.2)	29 (80.6)	7 (19.4)	0.020
Age in years, N (%)							
<1	13 (81.3)	3 (18.7)	11 (78.6)	3 (21.4)	2 (100)	0 (0)	>0.999
1-9.9	125 (93.3)	9 (6.7)	100 (95.2)	5 (4.8)	25 (86.2)	4 (13.8)	0.101
≥10	28 (87.5)	4 (12.5)	26 (96.3)	1 (3.7)	2 (40.0)	3 (60.0)	0.008
Sex, N (%)							
Male	102 (90.3)	11 (9.7)	84 (93.3)	6 (6.7)	18 (78.3)	5 (21.7)	0.045
Female	64 (92.8)	5 (7.2)	53 (94.6)	3 (5.4)	11 (84.6)	2 (15.4)	0.235
White blood cell count $\times 10^9$/L, N (%)							
<50	130 (97.0)	4 (3.0)	104 (97.2)	3 (2.8)	26 (96.3)	1 (3.7)	>0.999
≥50	36 (75.0)	12 (25.0)	33 (84.6)	6 (15.4)	3 (33.3)	6 (66.7)	0.004
Cytogenetics, N (%)							
Hyperdiploidy*	29 (96.7)	1 (3.3)	29 (96.7)	1 (3.3)	0 (0)	0 (0)	-
BCR-ABL1	7 (63.6)	4 (36.4)	7 (87.5)	1 (12.5)	0 (0)	3 (100)	0.024
*ETV6-RUNX1**	35 (100)	0 (0)	18 (100)	0 (0)	17 (100)	0 (0)	-
KMT2A-rearranged	12 (85.7)	2 (14.3)	9 (81.8)	2 (18.2)	3 (100)	0 (0)	>0.999
*TCF3-PBX1**	9 (90.0)	1 (10.0)	9 (90.0)	1 (10.0)	0 (0)	0 (0)	-
B-others	74 (90.2)	8 (9.8)	65 (94.2)	4 (5.8)	9 (69.2)	4 (30.8)	0.019
Risk group, N (%)							
Standard risk	73 (98.6)	1 (1.4)	57 (98.3)	1 (1.7)	16 (100)	0 (0)	>0.999
Intermediate risk	77 (97.5)	2 (2.5)	68 (98.6)	1 (1.4)	9 (90.0)	1 (10.0)	0.282
High risk	16 (55.2)	13 (44.8)	12 (63.2)	7 (36.8)	4 (40.0)	6 (60.0)	0.270

Statistics: Fisher's exact test. *No statistics are computed because CD9 or prednisone response is a constant.

or Dex (IC_{50}: 253 *vs.* 51,552 nM; *P*=0.024), respectively (Figure 2D). The overexpression system did not appear supraphysiologic, as reflected by the similar mRNA and total protein levels of CD9 in CD9-overexpressing cells and cells with inherently high CD9 expression. Yet, the sensitivity of CD9-overexpressing cells to GC was still lower than $CD9^{high}$ BCP-ALL lines (*Online Supplementary Figure 2A, B*). We further adopted a loss-of-function approach by transducing $CD9^{high}$ 697 cells with GFP-tagged CRISPR/Cas9 lentiviral vectors bearing non-targeting or CD9-targeting single-guide RNA (sgRNA), and generated GFP^+CD9^{high} and GFP^+CD9^{low} stable cells (Figure 2E). Consistent with our observation that low CD9 expression is linked to GC resistance, CD9 knockout significantly decreased the sensitivity of 697 cells to Pred (IC_{50}: 348 *vs.* 261 nM; *P*=0.002) or Dex (IC_{50}: 16.9 *vs.* 14.4 nM; *P*=0.003) compared with control $CD9^{high}$ cells (Figure 2F).

CD9 binds to the glucocorticoid receptor but does not affect its expression, phosphorylation or translocation

In order to assess whether CD9 alters GC sensitivity via the GC receptor, we first measured the basal expression of NR3C1 in BCP-ALL cell lines. NR3C1 protein was ubiquitously expressed in $CD9^{low}$ and $CD9^{high}$ lines despite their differential responses to GC (*Online Supplementary Figure S3A*). There was also no significant difference in the protein expression of NR3C1 between $CD9^+$ and $CD9^-$ patient samples (Figure 3A). Concordantly, *NR3C1* mRNA expression neither differed between $CD9^+$ and $CD9^-$ cases nor correlated with *CD9* mRNA levels (Figure 3B). There were also no significant differences in the expression of major *NR3C1* isoforms (GRα, GRβ and GRγ)[37] when stratified by CD9 status. Furthermore, hotspot *NR3C1* mutations associated with GC resistance (p.Y478C and p.R477H)[38] could not be detected in any BCP-ALL cell lines or samples employed in this study (*Online Supplementary Table S5*). Parental (*Online Supplementary Figure S3B*) or transduced BCP-ALL cells (*Online Supplementary Figure S3C*) also had no differences in NR3C1 protein expression upon GC treatment. Besides, GC-induced phosphorylation of NR3C1 at Ser211 and Ser 226[23] was competent in both $CD9^{low}$ and $CD9^{high}$ SEM cells (Figure 3C). Given that GC induce receptor cytoplasmic-nuclear shuttling,[14] we next evaluated the subcellular level of NR3C1 in transduced BCP-ALL cells. Cytoplasmic to nuclear translocation of NR3C1 was robust upon GC stimulation in both control and CD9-overexpressing SEM cells (Figure 3D) and similarly in the KOPN-8 and 697 systems (*Online Supplementary Figure S3D*). CD9 typically exerts its function by binding with other partner proteins,[24] we therefore performed co-immunoprecipitation assay and unexpectedly revealed the physical interaction of CD9 with NR3C1 in $CD9^{high}$ SEM cells (Figure 3E). This interaction diminished upon GC stimulation, possibly due to the partial detachment and translocation of NR3C1 into the nucleus. The CD9-NR3C1 complex was also found in BCP-ALL lines with inherently

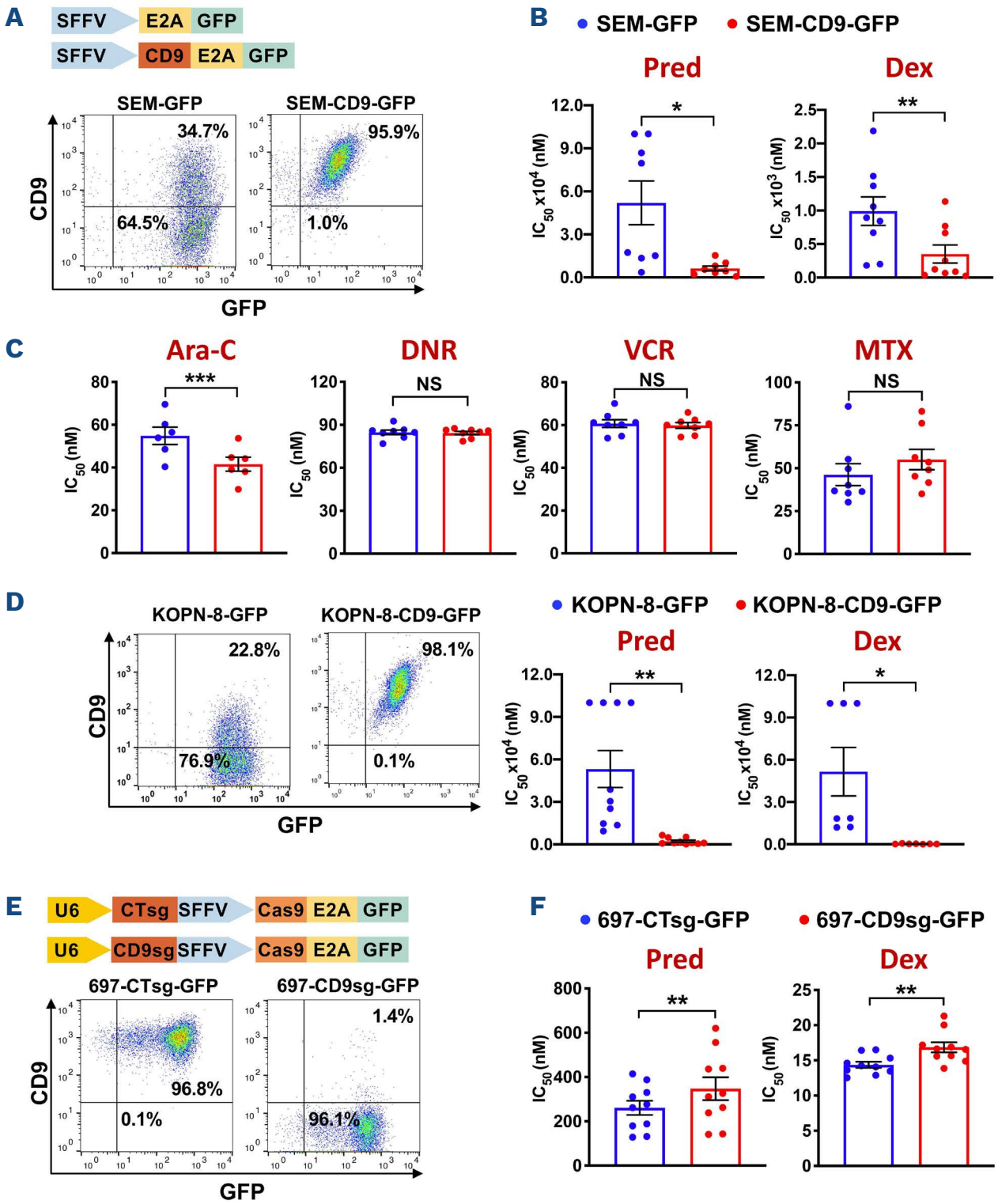

Figure 2. CD9 is functionally linked to glucocorticoid sensitivity. (A) Schematic diagram of lentiviral vectors for CD9 overexpression. Shown are representative flow cytometry plots depicting the expression of green fluorescence protein (GFP) and CD9 in transduced SEM cells after puromycin selection. (B) Differential sensitivity of control SEM-GFP and experimental SEM-CD9-GFP cells to glucocorticoids (N=8-9). (C) Responses of transduced SEM cells to other chemotherapeutic agents (N=6-8). (D) Representative flow cytometry plots showing the expression of GFP and CD9 in stably transduced KOPN-8 cells, and their sensitivity to glucocorticoids (N=7-10). (E) Schematic diagram of lentiviral vectors for CD9 knockout. Shown are representative flow cytometry plots depicting the expression of GFP and CD9 in transduced 697 cells after fluorescence-activated cell sorting. (F) Differential sensitivity of control 697-CTsg-GFP and experimental 697-CD9sg-GFP cells to glucocorticoids (N=10). Statistics: two-tailed, paired Student's *t* test. **P*<0.05, ***P*<0.01, ****P*<0.001, NS: not significant. SFFV: spleen focus-forming virus U3 promoter; E2A: a self-cleavage site derived from equine rhinitis A virus; U6: RNA polymerase III promoter; sg: single-guide RNA; Cas9: CRISPR associated protein 9.

high CD9 expression, and precipitated together with well-known CD9 interactors EWI-2 and CD81 within the TEM (*Online Supplementary Figure S4*).

CD9 enhances transcription of glucocorticoid-responsive genes

In order to identify the downstream gene signatures underpinning GC sensitivity, we performed RNA sequencing (RNA-seq) on $CD9^{high}$ and $CD9^{low}$ SEM cells upon GC exposure. After an 8-hour Dex treatment, more differentially expressed genes (DEG) were found in $CD9^{high}$ than $CD9^{low}$ cells (110 *vs.* 82; Figure 4A). Venn analysis showed that 75 DEG were commonly regulated by Dex in both $CD9^{high}$ and $CD9^{low}$ cells, whereas 35 DEG were exclusively altered in $CD9^{high}$ cells (Figure 4B). The complete list of DEG is shown in *Online Supplementary Table S6*, where 28 of

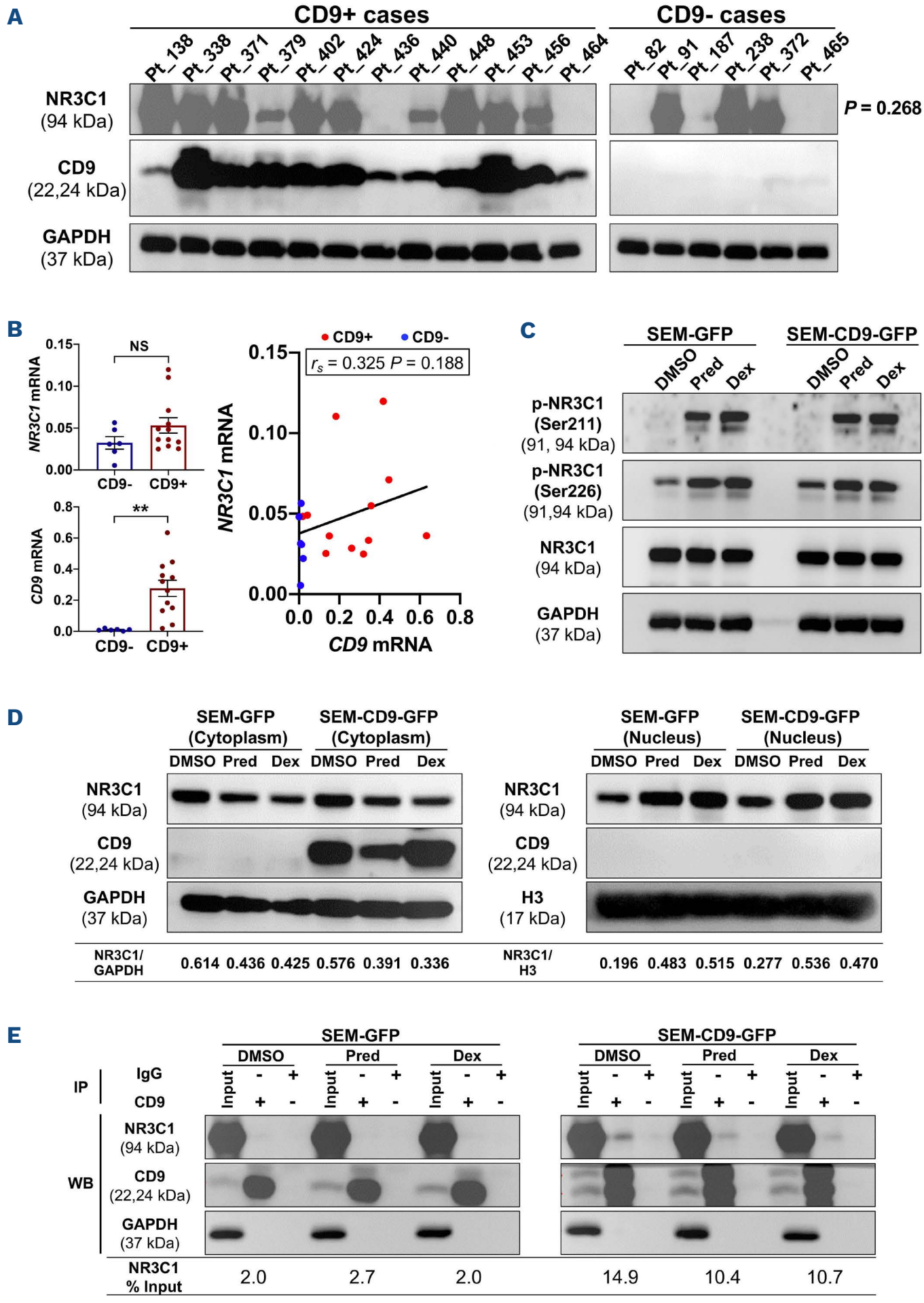

Figure 3. CD9 binds to NR3C1 but does not affect its expression, phosphorylation and nuclear translocation. (A) Expression of NR3C1 in CD9$^+$ (N=12) or CD9$^-$ (N=6) B-cell precursor acute lymphoblastic leukemia samples as revealed by western blotting, with GAPDH as the internal control. (B) *NR3C1* and *CD9* mRNA expression in patient samples relative to *GAPDH* and their correlation. (C) Phosphorylation status of NR3C1 in SEM-GFP and SEM-CD9-GFP cells after an 8-hour exposure to dimethyl sulfoxide (DMSO), prednisolone (Pred) (50 μM) or dexamethasone (Dex) (1 μM). (D) NR3C1 protein level in fractionated lysates of SEM-GFP and SEM-CD9-GFP cells with or without exposure to glucocorticoids (Pred, 50 μM; Dex, 1 μM for 8 hours). NR3C1/GAPDH intensity ratios for the cytoplasmic fraction or NR3C1/H3 ratios for the nuclear fraction are shown. (E) Lysates from SEM-GFP and SEM-CD9-GFP after glucocorticoid treatments (Pred, 50 μM; Dex, 1 μM for 8 hours) were immunoprecipitated with control IgG2b or anti-CD9, and probed with antibodies against NR3C1, CD9 or GAPDH after electrophoresis. The levels of co-precipitated NR3C1 normalized to lysate input in respective treatments are shown. All presented images are representative of at least 3 independent experiments. Statistics: (A) Fisher's exact test; (B, left) two-tailed, unpaired Student's *t* test; (B, right) Spearman's correlation. ***P*<0.01, NS: not significant.

them are known GC-responsive genes. We next validated three DEG, including *ZBTB16* (PLZF), *TSC22D3* (GILZ) and *BCL2L11* (BIM) that are well known GC-responsive genes participating in GC-induced apoptosis or cell cycle progression.[21,39,40] By quantitative polymerase chain reaction (qPCR), we found that the magnitude of their induction was significantly higher in CD9^{high} cells (P<0.05; Figure 4C). Given that CD9 illuminates a more robust GC-induced gene transcription program despite intact NR3C1 nuclear translocation, we further performed chromatin immunoprecipitation sequencing (ChIP-seq) to assess NR3C1 binding to GC-responsive genes. In both CD9^{high} and CD9^{low} SEM cells, we detected distinct peaks in the glucocorticoid response elements (GRE) of *TSC22D3* and *ZBTB16* upon Dex treatment (Figure 4D), indicating that DNA binding of translocated NR3C1 was competent.

MEK inhibition preferentially increases the susceptibility of CD9^{low} B-cell precursor acute lymphoblastic leukemia cells to glucocorticoids

Given that constitutive activation of the MAPK pathway is associated with GC resistance,[17] we assessed the synergism of GC with the MEK inhibitor trametinib in CD9^{+} and CD9^{-} BCP-ALL cells. Trametinib exhibited a strong synergy with Pred or Dex in CD9^{low} SEM and KOPN-8 cells (excess over Bliss score >0) but antagonism in CD9^{high} RS4;11 and BV-173 cells (excess over Bliss score <0) (*Online Supplementary Figure S5A*). Furthermore, in SEM and KOPN-8 cells, CD9 overexpression consistently reduced the synergy between GC and trametinib (*Online Supplementary Figure S5B*). These phenomena were successfully recapitulated with animal modeling. In CD9^{low} SEM but not CD9^{high} BV-173 xenografts, combined treatment with Dex and trametinib

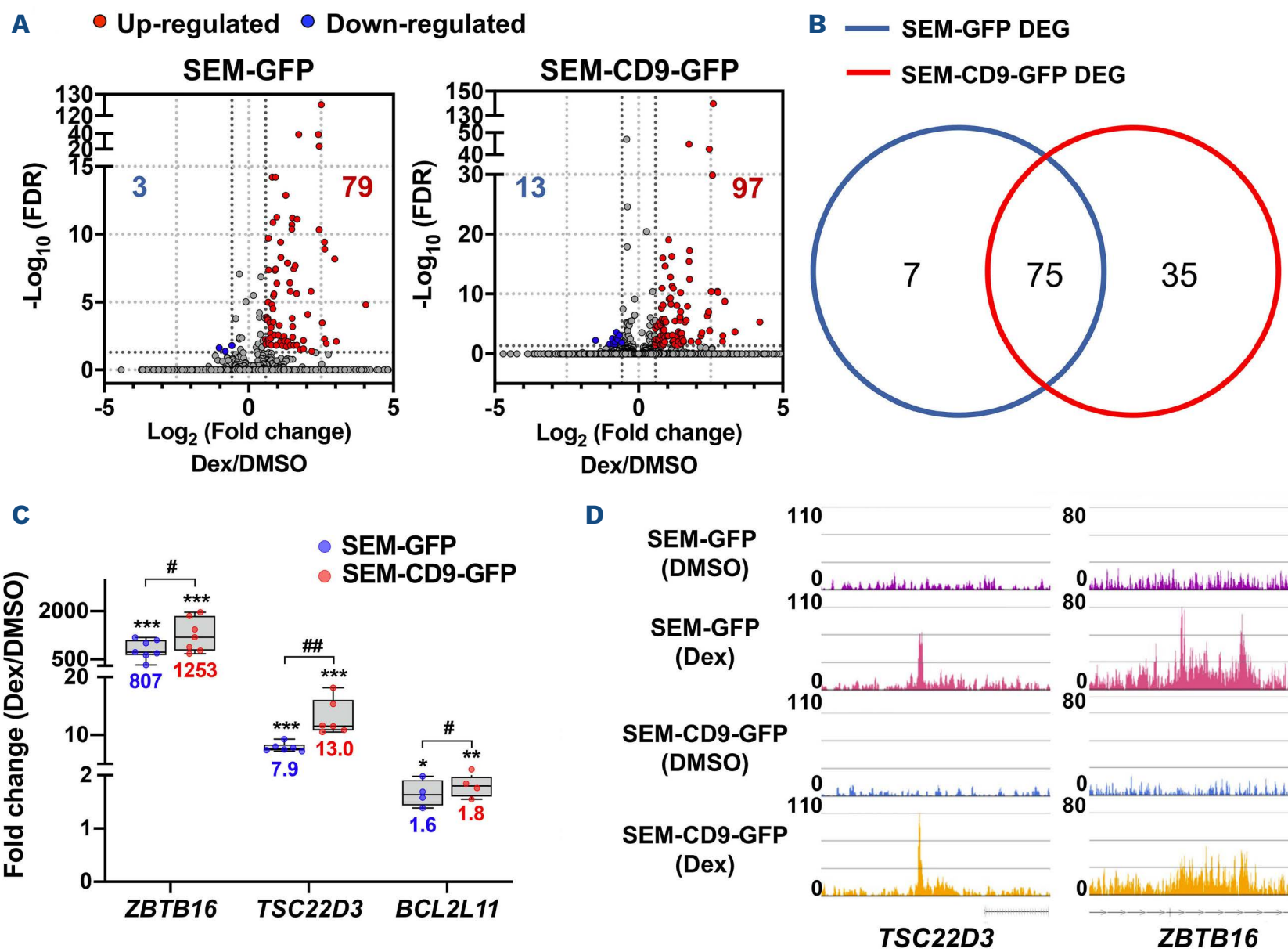

Figure 4. CD9 potentiates the expression of glucocorticoid-responsive genes. SEM-GFP and SEM-CD9-GFP cells were exposed to dexamethasone (Dex) (1 μM) for 8 hours and subjected to RNA sequencing (RNA-seq), quantitative real-time polymerase chain reaction (qRT-PCR) and chromatin immunoprecipitation sequencing (ChIP-seq). (A) Volcano plots showing the differentially expressed genes (DEG) in Dex-treated SEM-GFP (N=82) and SEM-CD9-GFP cells (N=110) identified by RNA-seq. Suppressed DEG are indicated in blue, and augmented DEG in red. (B) Venn diagram showing the number of overlapping and exclusive DEG in SEM-GFP and SEM-CD9-GFP cells induced by Dex. (C) qRT-PCR validation of selected DEG (N=4-7). The indicated values are the fold induction by Dex over dimethyl sulfoxide (DMSO). Statistics: two-tailed, paired Student's *t* test comparing (i) the changes in gene expression upon Dex treatment of SEM-GFP (blue) or SEM-CD9-GFP cells (red), *P<0.05, **P<0.01, ***P<0.001; and (ii) the magnitudes of glucocorticoid-mediated gene induction between SEM-GFP and SEM-CD9-GFP cells (blue *vs.* red), $^{\#}P$<0.05, $^{\#\#}P$<0.01. (D) Individual NR3C1 ChIP-seq tracks for selected glucocorticoid-responsive genes.

effectively reduced systemic and medullary leukemic load when compared to single-agent treatments (P<0.05; Figure 5A). In patient samples, despite their differences in GC sensitivity, we neither observed significant differences in the activation status of the MAPK pathway components between CD9$^+$ and CD9$^-$ cases (*Online Supplementary Figure S6A*) nor their correlation with trametinib sensitivity (*Online Supplementary Figure S6B*). Consistent with the observations in BCP-ALL cell lines, trametinib only exhibited synergy with Dex in CD9$^-$ but additivity or antagonism in CD9$^+$ cases (Figure 5B), suggesting trametinib may preferentially benefit CD9$^-$ patients. Given that STAT5 and ERK are segregated in BCP-ALL,[41] CD9$^+$ lymphoblasts may escape from the trametinib/GC combination by compensatory activation of the STAT pathway. Coincidentally, the gain of CD9 induced an exclusive upregulation of *STAT5A* in Dex-treated SEM cells (P=0.023; Figure 5C). *Ex vivo* drug testing showed that the JAK inhibitor ruxolitinib tended to provide an additional degree of leukemia suppression in the background of trametinib/Dex combination in CD9$^+$ cases (Figure 5D).

Discussion

In this study, we have established a previously unknown linkage between CD9 and GC sensitivity in pediatric BCP-ALL and informed pharmacologic approaches guided by CD9 status to reverse GC resistance. Our data not only uncover a new biological function of CD9 but also implicate improved strategies for the management of this childhood malignancy.

By drug sensitivity profiling of BCP-ALL cells, we identified an apparent association of CD9 negativity with GC resistance. This phenomenon is specific to GC but not to other cytotoxic agents. Notably, the respective reversal and acquisition of relative GC resistance upon CD9 overexpression and knockout further provided definitive proof for its genuine control of GC susceptibility. Similar to its well-documented oncogenic and tumor suppressive functions,[25] CD9 can exert context-dependent regulation of drug sensitivity in different cancer types. In multiple myeloma, downregulation of CD9 by DNA methylation was functionally linked to bortezomib resistance.[42] In contrast, increased expression of CD9 in breast cancer was responsible for resistance to doxorubicin and 5-fluorouracil by modulating the crosstalk between tumor cells and MSC.[43] Likewise, preferential expression of CD9 in metastatic small cell lung cancer mediated resistance to etoposide and cisplatin *via* activation of β1 integrin.[44] These findings, together with ours, illustrate the complex nature of CD9 in regulating drug responses, where both cell adhesion-dependent and -independent mechanisms may concurrently exist. Indeed, the linkage of CD9 to GC resistance was consistently observed in both leukemia monocultures and MSC co-cultures, suggesting that the effects of CD9 on GC responsiveness in BCP-ALL are possibly regulated by cell-intrinsic mechanisms.

In a cohort of pediatric BCP-ALL patients, we found that CD9 negativity independently predicted poor Pred responses. Interestingly, Pred non-responders were mostly enriched in CD9$^-$ patients with older age, higher white cell count, male sex and *BCR-ABL1*. Although these are also recognized risk factors for poor Pred response that might potentially confound the interpretation, CD9 negativity still stood out as an independent predictive factor in multivariate analyses. Given that some consortia have adopted multiple drug induction without Pred prephase in newer treatment protocols,[4,45] CD9 expression status at diagnosis could therefore serve as a surrogate marker for initial risk stratification. Our previous study contradictorily identified that CD9 positivity was associated with inferior survival in pediatric BCP-ALL.[27] This could be ascribed to more CD9$^-$ patients being stratified into the high-risk group due to inadequate Pred responses to receive intensive multiagent chemotherapy. Thus, the negative impact of GC resistance might have been overcome by other subsequent chemotherapeutic agents. Notably, CD9 also strongly predicted poor Pred responses in patients with unclassified BCP-ALL subtypes, as limited by our cytogenetics detection panel. With advances in deep genomic profiling,[46] it will be important to identify the exact molecular BCP-ALL subtypes that are specifically influenced by CD9 through a larger patient cohort. In contrast to BCP-ALL where CD9$^+$ cases predominated the patient population, the majority of T-ALL cases were CD9$^-$ as shown by our recent nationwide study.[28] Since GC resistance is a particular obstacle for T-ALL treatment,[47] it will be imperative to investigate whether GC responses are also shaped by CD9 in this leukemia type that could potentially inform new intervening strategies.

In pediatric ALL, mutations of the GC receptor *NR3C1* were rarely detected,[48,49] and evidence documenting the association between its expression and GC response appears conflicting.[50,51] Consistent with these findings, we observed ubiquitous mRNA and protein expression of NR3C1 in GC-sensitive CD9^{high} and GC-resistant CD9^{low} BCP-ALL cells. The same was also true for *NR3C1* isoforms and its mutational status. In addition, the phosphorylation of NR3C1 was robust, indicating that CD9 regulates GC sensitivity through NR3C1 expression-, mutation- and activation-independent mechanisms. In line with the fact that tetraspanin family proteins typically act by forming microdomains with other partner proteins,[24] we reported for the first time that CD9 physically interacted with NR3C1 within the TEM. However, this interaction did not alter the nuclear translocation of NR3C1 and subsequent binding to GRE upon GC stimulation despite an elevated transcriptional program in the background of CD9. While the enhanced GC sensitivity in CD9^{high} cells could potentially

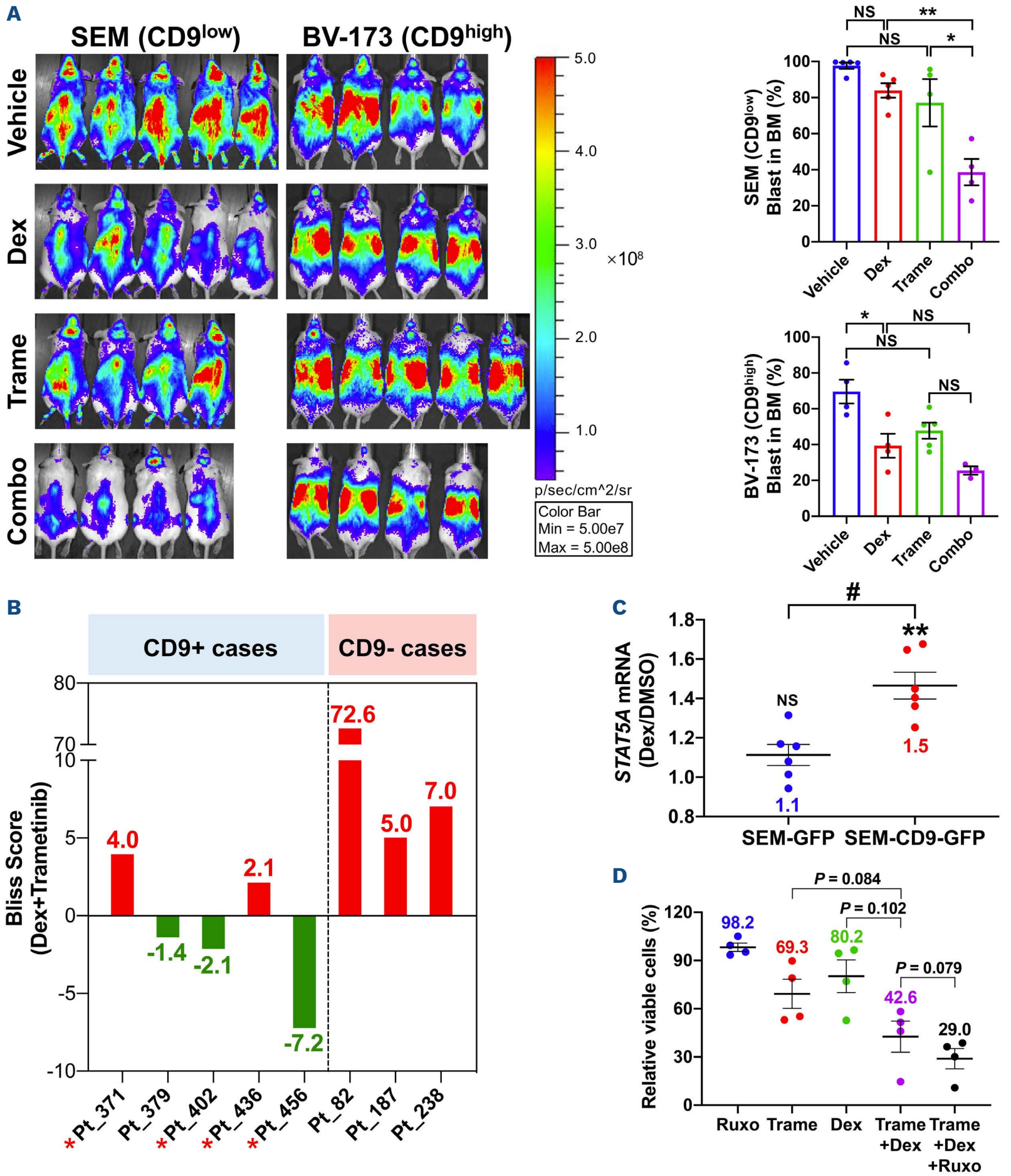

Figure 5. MEK inhibition restores the susceptibility of CD9^{low} cells to glucocorticoids. (A) NSG mice were infused with luciferase-expressing CD9^{low} SEM or CD9^{high} BV-173 cells (1×10^6/mouse), and randomized to receive daily treatment of vehicle control, dexamethasone (Dex) (5 mg/kg by intraperitoneal injection), trametinib (5 mg/kg by oral gavage) or their combination for 2 weeks (5 days on, 2 days off) starting on day 3 after leukemic cell infusion (4-5 mice/group). (Left) Systematic leukemic load was monitored by bioluminescence imaging when animals in the vehicle groups reached humane endpoints (day 33 for SEM; day 28 for BV-173). (Right) Concurrent enumeration of leukemic blasts in the bone marrow by flow cytometry. Blasts were defined as human CD45$^+$CD19$^+$ cells. (B) Mode of trametinib/Dex interactions in CD9$^+$ (N=5) and CD9$^-$ (N=3) samples. The Bliss scores of individual samples are indicated, with red bars indicating drug synergy and green bars representing drug antagonism. Asterisks denote samples chosen for JAK-STAT inhibition experiments. (C) *STAT5A* expression in SEM-GFP and SEM-CD9-GFP cells (N=6). The indicated values are the fold induction by Dex over dimethyl sulfoxide (DMSO). (D) Lymphoblasts from CD9$^+$ cases (N=4) were treated with single agent ruxolitinib (0.1 nM), trametinib (10 nM), Dex (1-10 nM) or their combinations for 96 hours in mesenchymal stem cell (MSC) co-cultures. Shown are the mean percentage of viable cells relative to DMSO controls. Statistics: (A) two-tailed, unpaired Student's *t* test; (C, D) two-tailed, paired Student's *t* test. $^*P$<0.05, $^{**}P$<0.01, $^{\#}P$<0.05, NS: not significant.

be explained by upregulation of proapoptotic genes such as BIM,[21] the mechanisms underlying how CD9 potentiates their transcription are still elusive and unlikely to be a direct consequence of altered NR3C1 activity. Given that NR3C1 is regulated by multiple signals (ligands, DNA-binding sequences, post-translational modifications and non-NR3C1 transcriptional regulatory factors),[52] one future direction is to map the whole spectrum of CD9 binding proteins within the TEM, coupled with a genome-scale knockout screen to functionally identify the partner(s) that are regulatory elements of GC-driven gene transcription.

Restoring GC sensitivity by enhancing CD9 expression, however, would be undesirable as it may at the same time increase leukemia aggressiveness.[27,28] Emerging studies suggest that GC resistance in BCP-ALL is mediated by constitutive activation of MAPK signaling.[17] In connection, the MEK inhibitor trametinib was recently approved for solid tumors with BRAF mutations,[53] and is now under clinal evaluation in combination with dexamethasone and chemotherapy for children with relapsed or refractory ALL or lymphoblastic lymphoma (*clinicaltrials gov. Identifier: NCT05658640*). However, MEK or ERK phosphorylation varied extensively among patients and alone could not predict sensitivity to MEK inhibitors in multiple cancer types,[54,55] including BCP-ALL as shown in this study. Our data indeed showed that trametinib only exhibited strong synergism with GC in $CD9^-$ over $CD9^+$ BCP-ALL, suggesting that CD9 status could serve as a biomarker to identify patients who are most likely to benefit from this intervention. On the other hand, the lack of efficacy to the trametinib/GC combo in $CD9^+$ cases might originate from activation of parallel signaling pathways that cause intrinsic or adaptive resistance,[56,57] where GC-induced upregulation of *STAT5A* was evidenced only in the presence of CD9. The addition of ruxolitinib to $CD9^+$ lymphoblasts appeared to provide extra benefit on top of combinatorial trametinib/GC, suggesting a third drug targeting the JAK-STAT axis may be necessary to profit poor Pred responders with a $CD9^+$ phenotype.

Disclosures

No conflicts of interest to disclose.

Contributions

CZ, KYYC, WHN, JTKC, QS, HW, PYC, PYL, SPF, and GL performed the experiments and analyzed the data. FWTC, and AWKL provided clinical samples and obtained patient consent. XBZ, ENYP, JHF, YLT, XQL, LBH, WK, PMKT, JH, CC, JD, EM, JC, YL, SS, and JJY provided advice on study design, contributed to essential laboratory reagents, solicited clinical data, and edited the manuscript. PMPY, CKL, and KTL conceived the study, interpreted the data, wrote the manuscript, and contributed to research funding. All authors have reviewed and approved the final paper.

Funding

This study was supported by the Bone Marrow Transplant Fund, Hong Kong (project no. 7105113); Children's Cancer Foundation, Hong Kong (project no. 7104593); HOPE Research Seed Fund, The Chinese University of Hong Kong, Hong Kong (project no. HOPE-007); Sanming Project of Medicine, Shenzhen, China (project no. SZSM202011004); IdeaBooster Fund, The Chinese University of Hong Kong, Hong Kong (project no. IDBF23MED11); Ministry of Health, Czech Republic (AZV no. NU23-05-00353); and Direct Grant for Research, The Chinese University of Hong Kong, Hong Kong (project no. 4054491). The funding bodies were not involved in the study design, the collection, analysis, and interpretation of data, or the decision to submit the manuscript for publication.

Data-sharing statement

Sequencing data of BCP-ALL cell lines were deposited in Gene Expression Omnibus (GEO; accession no. GSE220979). Sequencing data of patient samples are available from the corresponding author on reasonable request. The data are not publicly available due to privacy or ethical restrictions.

References

1. Miranda-Filho A, Piñeros M, Ferlay J, Soerjomataram I, Monnereau A, Bray F. Epidemiological patterns of leukaemia in 184 countries: a population-based study. Lancet Haematol. 2018;5(1):e14-e24.
2. Hunger SP, Mullighan CG. Acute lymphoblastic leukemia in children. N Engl J Med. 2015;373(16):1541-1552.
3. Pui CH, Yang JJ, Hunger SP, et al. Childhood acute lymphoblastic leukemia: progress through collaboration. J Clin Oncol. 2015;33(27):2938-2948.
4. Tang J, Yu J, Cai J, et al. Prognostic factors for CNS control in children with acute lymphoblastic leukemia treated without cranial irradiation. Blood. 2021;138(4):331-343.
5. Bhojwani D, Pui CH. Relapsed childhood acute lymphoblastic leukaemia. Lancet Oncol. 2013;14(6):e205-e217.
6. Hunger SP, Raetz EA. How I treat relapsed acute lymphoblastic leukemia in the pediatric population. Blood. 2020;136(16):1803-1812.
7. Li CK, Chik KW, Ha SY, et al. Improved outcome of acute lymphoblastic leukaemia treated by delayed intensification in Hong Kong children: HKALL97 study. Hong Kong Med J. 2006;12(1):33-39.
8. Stary J, Zimmermann M, Campbell M, et al. Intensive chemotherapy for childhood acute lymphoblastic leukemia: results of the randomized intercontinental trial ALL IC-BFM 2002. J Clin Oncol. 2014;32(3):174-184.
9. Cui L, Li ZG, Chai YH, et al. Outcome of children with newly diagnosed acute lymphoblastic leukemia treated with CCLG-ALL 2008: the first nation-wide prospective multicenter study

in China. Am J Hematol. 2018;93(7):913-920.
10. Campbell M, Kiss C, Zimmermann M, et al. Childhood acute lymphoblastic leukemia: results of the randomized acute lymphoblastic leukemia Intercontinental-Berlin-Frankfurt-Münster 2009 trial. J Clin Oncol. 2023;41(19):3499-3511.
11. Inaba H, Pui CH. Glucocorticoid use in acute lymphoblastic leukaemia. Lancet Oncol. 2010;11(11):1096-1106.
12. Schrappe M, Aricò M, Harbott J, et al. Philadelphia chromosome-positive (Ph+) childhood acute lymphoblastic leukemia: Good initial steroid response allows early prediction of a favorable treatment outcome. Blood. 1998;92(8):2730-2741.
13. Dördelmann M, Reiter A, Borkhardt A, et al. Prednisone response is the strongest predictor of treatment outcome in infant acute lymphoblastic leukemia. Blood. 1999;94(4):1209-1217.
14. Vandewalle J, Luypaert A, De Bosscher K, Libert C. Therapeutic mechanisms of glucocorticoids. Trends Endocrinol Metab. 2018;29(1):42-54.
15. Wandler AM, Huang BJ, Craig JW, et al. Loss of glucocorticoid receptor expression mediates in vivo dexamethasone resistance in T-cell acute lymphoblastic leukemia. Leukemia. 2020;34(8):2025-2037.
16. Mullighan CG, Zhang J, Kasper LH, et al. CREBBP mutations in relapsed acute lymphoblastic leukaemia. Nature. 2011;471(7337):235-239.
17. Jones CL, Gearheart CM, Fosmire S, et al. MAPK signaling cascades mediate distinct glucocorticoid resistance mechanisms in pediatric leukemia. Blood. 2015;126(19):2202-2212.
18. Real PJ, Tosello V, Palomero T, et al. γ-secretase inhibitors reverse glucocorticoid resistance in T cell acute lymphoblastic leukemia. Nat Med. 2009;15(1):50-58.
19. Xie M, Yang A, Ma J, et al. Akt2 mediates glucocorticoid resistance in lymphoid malignancies through FoxO3a/Bim axis and serves as a direct target for resistance reversal. Cell Death Dis. 2019;9(10):1013.
20. Poulard C, Kim HN, Fang M, et al. Relapse-associated AURKB blunts the glucocorticoid sensitivity of B cell acute lymphoblastic leukemia. Proc Natl Acad Sci U S A. 2019;116(8):3052-3061.
21. Jing D, Huang Y, Liu X, et al. Lymphocyte-specific chromatin accessibility pre-determines glucocorticoid resistance in acute lymphoblastic leukemia. Cancer Cell. 2018;34(6):906-921.
22. Olivas-Aguirre M, Torres-López L, Pottosin I, Dobrovinskaya O. Overcoming glucocorticoid resistance in acute lymphoblastic leukemia: repurposed drugs can improve the protocol. Front Oncol. 2021;11:617937.
23. Piovan E, Yu J, Tosello V, et al. Direct reversal of glucocorticoid resistance by AKT inhibition in acute lymphoblastic leukemia. Cancer Cell. 2013;24(6):766-776.
24. Hemler ME. Tetraspanin functions and associated microdomains. Nat Rev Mol Cell Biol. 2005;6(10):801-811.
25. Zöller M. Tetraspanins: push and pull in suppressing and promoting metastasis. Nat Rev Cancer. 2009;9(1):40-55.
26. Leung KT, Chan KY, Ng PC, et al. The tetraspanin CD9 regulates migration, adhesion, and homing of human cord blood CD34+ hematopoietic stem and progenitor cells. Blood. 2011;117(6):1840-1850.
27. Leung KT, Zhang C, Chan KY, et al. CD9 blockade suppresses disease progression of high-risk pediatric B-cell precursor acute lymphoblastic leukemia and enhances chemosensitivity. Leukemia. 2020;34(3):709-720.
28. Leung KT, Cai J, Liu Y, et al. Prognostic implications of CD9 in childhood acute lymphoblastic leukemia: insights from a nationwide multicenter study in China. Leukemia. 2024;38(2):250-257.
29. Chan KYY, Zhang C, Wong YTS, et al. R4 RGS proteins suppress engraftment of human hematopoietic stem/progenitor cells by modulating SDF-1/CXCR4 signaling. Blood Adv. 2021;5(21):4380-4392.
30. Lee SHR, Yang W, Gocho Y, et al. Pharmacotypes across the genomic landscape of pediatric acute lymphoblastic leukemia and impact on treatment response. Nat Med. 2023;29(1):170-179.
31. Wang H, Chan KYY, Cheng CK, et al. Pharmacogenomic profiling of pediatric acute myeloid leukemia to identify therapeutic vulnerabilities and inform functional precision medicine. Blood Cancer Discov. 2022;3(6):516-535.
32. Bliss CI. The toxicity of poisons applied jointly. Ann Appl Biol. 1939;26(3):585-615.
33. Liu T, Rao J, Hu W, et al. Distinct genomic landscape of Chinese pediatric acute myeloid leukemia impacts clinical risk classification. Nat Commun. 2022;13(1):1640.
34. Zhang C, Zhang B, Lin L-L, Zhao S. Evaluation and comparison of computational tools for RNA-seq isoform quantification. BMC Genomics. 2017;18(1):583.
35. Verbeke D, Demeyer S, Prieto C, et al. The XPO1 inhibitor KPT-8602 synergizes with dexamethasone in acute lymphoblastic leukemia. Clin Cancer Res. 2020;26(21):5747-5758.
36. Kerstjens M, Pinhancos SS, Castro PG, et al. Trametinib inhibits RAS-mutant MLL-rearranged acute lymphoblastic leukemia at specific niche sites and reduces ERK phosphorylation in vivo. Haematologica. 2018;103(4):e147-e150.
37. Haarman EG, Kaspers GJL, Pieters R, Rottier MMA, Veerman AJP. Glucocorticoid receptor alpha, beta and gamma expression vs in vitro glucocorticod resistance in childhood leukemia. Leukemia. 2004;18(3):530-537.
38. Liu H, Li Z, Qiu F, et al. Association between NR3C1 mutations and glucocorticoid resistance in children with acute lymphoblastic leukemia. Front Pharmacol. 2021;12:634956.
39. Wasim M, Carlet M, Mansha M, et al. PLZF/ZBTB16, a glucocorticoid response gene in acute lymphoblastic leukemia, interferes with glucocorticoid-induced apoptosis. J Steroid Biochem Mol Biol. 2010;120(4-5):218-227.
40. Riccardi C, Cifone MG, Migliorati G. Glucocorticoid hormone-induced modulation of gene expression and regulation of T-cell death: role of GITR and GILZ, two dexamethasone-induced genes. Cell Death Differ. 1999;6(12):1182-1189.
41. Chan LN, Murakami MA, Robinson ME, et al. Signalling input from divergent pathways subverts B cell transformation. Nature. 2020;583(7818):845-851.
42. Hu X, Xuan H, Du H, Jiang H, Huang J. Down-regulation of CD9 by methylation decreased bortezomib sensitivity in multiple myeloma. PloS One. 2014;9(5):e95765.
43. Ullah M, Akbar A, Ng NN, Concepcion W, Thakor AS. Mesenchymal stem cells confer chemoresistance in breast cancer via a CD9 dependent mechanism. Oncotarget. 2019;10(37):3435-3450.
44. Kohmo S, Kijima T, Otani Y, et al. Cell surface Tetraspanin CD9 mediates chemoresistance in small cell lung cancer. Cancer Res. 2010;70(20):8025-8035.
45. Maloney KW, Devidas M, Wang C, et al. Outcome in children with standard-risk B-cell acute lymphoblastic leukemia: results of children's oncology group trial AALL0331. J Clin Oncol. 2020;38(6):602-612.
46. Brady SW, Roberts KG, Gu Z, et al. The genomic landscape of

pediatric acute lymphoblastic leukemia. Nat Genet. 2022;54(9):1376-1389.
47. De Smedt R, Morscio J, Goossens S, Van Vlierberghe P. Targeting steroid resistance in T-cell acute lymphoblastic leukemia. Blood Rev. 2019;38:100591.
48. Ding LW, Sun QY, Tan KT, et al. Mutational landscape of pediatric acute lymphoblastic leukemia. Cancer Res. 2017;77(2):390-400.
49. Oshima K, Khiabanian H, da Silva-Almeida AC, et al. Mutational landscape, clonal evolution patterns, and role of RAS mutations in relapsed acute lymphoblastic leukemia. Proc Natl Acad Sci. 2016;113(40):11306-11311.
50. Lauten M, Cario G, Asgedom G, Welte K, Schrappe M. Protein expression of the glucocorticoid receptor in childhood acute lymphoblastic leukemia. Haematologica. 2003;88(11):1253-1258.
51. Koga Y, Matsuzaki A, Suminoe A, Hattori H, Kanemitsu S, Hara T. Differential mRNA expression of glucocorticoid receptor α and β is associated with glucocorticoid sensitivity of acute lymphoblastic leukemia in children. Pediatr Blood Cancer. 2005;45(2):121-127.
52. Weikum ER, Knuesel MT, Ortlund EA, Yamamoto KR. Glucocorticoid receptor control of transcription: precision and plasticity via allostery. Nat Rev Mol Cell Biol. 2017;18(3):159-174.
53. Dummer R, Long GV, Robert C, et al. Randomized phase III trial evaluating spartalizumab plus dabrafenib and trametinib for BRAF V600-mutant unresectable or metastatic melanoma. J Clin Oncol. 2022;40(13):1428-1438.
54. Rožanc J, Sakellaropoulos T, Antoranz A, et al. Phosphoprotein patterns predict trametinib responsiveness and optimal trametinib sensitisation strategies in melanoma. Cell Death Differ. 2019;26(8):1365-1378.
55. Wagle M-C, Kirouac D, Klijn C, et al. A transcriptional MAPK pathway activity score (MPAS) is a clinically relevant biomarker in multiple cancer types. NPJ Precis Oncol. 2018;2(1):7.
56. Perna D, Karreth FA, Rust AG, et al. BRAF inhibitor resistance mediated by the AKT pathway in an oncogenic BRAF mouse melanoma model. Proc Natl Acad Sci U S A. 2015;112(6):E536-545.
57. Vultur A, Villanueva J, Krepler C, et al. MEK inhibition affects STAT3 signaling and invasion in human melanoma cell lines. Oncogene. 2014;33(14):1850-1861.